AN EFFICIENT ALGORITHM FOR GENERAL 3D-SEISMIC BODY WAVES
(SSP AND VSP APPLICATIONS)

Mohammad Kamal GhasemAl-Askari
Petroleum University of Technology, askari5027@yahoo.com

Seyed Jalaladdin Hashemi
PUT and Islamic Azad University-Ahvaz Branch, hashemi_sj@put.ac.ir

(Received: Oct. 25, 2003)

Abstract The ray series method may be generalized using a ray centered coordinate system for general 3D-heterogeneous media. This method is useful for Amplitude Versus Offset (AVO) seismic modeling, seismic analysis, interpretational purposes, and comparison with seismic field observations.
For each central ray (constant ray parameter), the kinematic (the eikonal) and dynamic ray tracing system of equations are numerically solved. Then, the ray impulse and the ray synthetic seismograms are efficiently computed. The reflected, refracted, critically diffracted, multiples and converted P-waves and/or S-waves are computed and evaluated at the ray endpoints. The central Ray Method application to two-dimensional models are investigated and comparison with seismic wave field are successfully done. Two examples of the ray field and synthetic seismograms for the complex models are presented here both for *surface seismic profiling* (SSP) and *vertical seismic profiling* (VSP).

Keywords 3D-Seismic, SSP, VSP, synthetic seismograms, dynamic ray tracing.

چکیده روش سری های پرتو با بکارگیری دستگاه مختصات پرتو مرکزی برای محیط های سه بعدی-ناهمگن تعمیم داده شده است. این روش برای تفسیر و مدلسازی لرزه ای دامنه برحسب فاصله از چشمه (آ، وی، او) و مقایسه با داده های لرزه ای صحرائی بکار می رود.
دستگاه معادلات پرتو بصورت سینماتیکی و دینامیکی مسیر پرتو برای هر پرتو مرکزی به روش محاسبات عددی حل می شود. سپس نگاشت مصنوعی اولیه و نگاشت های آمیخته شده با الگوریتمی که محاسبات را تسریع می نماید حل می شود. امواج بازتابی، انکساری، پراکنشی و چند گانه و بخصوص امواج تبدیلی و برشی در نقطه انتهایی هر پرتو محاسبه می شود. روش پرتو مرکزی در مدل های دو بعدی و سه بعدی محاسبه شده و نتایج با داده های صحرائی مقایسه گردید که نتایج قابل قبولی بدست داده است. چند مثال از مدلسازی روش پرتو و محاسبات نگاشت های مصنوعی برای مدل های ساده و مدل های پیچیده محاسبه شده و با هم مقایسه گردیده است. این روش را می توان برای مدلسازی لرزه ای سطحی و عمودی مورد استفاده قرار داد.

1. INTRODUCTION

Synthetic seismograms introduced in this paper, is an aid to understand and interpret wave propagation phenomena through realistic earth models for both SSP and VSP data.

Many techniques are now available for the computation of synthetic seismograms. One of the fast technique which can be easily applied to elastic heterogeneous media is the ray method and its various modifications[1-3]. A similar approach to the ray method, with extension to wavefields in

laterally heterogeneous media, the so called Gaussian Beam Method was developed by Cerveny[4] and Cerveny et. al.,[4, 5].
The central ray technique is used to construct synthetic seismograms with non-zero torsion[6], as in Asymptotic Ray Theory (ART), the whole wavefield is decomposed into small contributions corresponding to individual rays. The central ray information is taken and the Gaussian distribution is applied, such that each ray tube converges at the receiver with a finite number of iterations. This method can be used to compute synthetic seismograms for curved interfaces, laterally heterogeneous media, and block structures, both for SSP and VSP seismic applications.
VSP is one of the fast and high resolution method used in exploration of oil and gas. It consists of two parts:
a) recording borehole VSP data,
b) data simulation processing .
Simultaneous interpretation of synthetic and real VSP data helps the geophysicist to better understand the links between SSP and downhole well logs.
In this paper the application of the Central Ray Method to two-dimensional models are investigated and the comparison with seismic wave field are successfully done.
Zednik[7] has generated a package for the three-component ray-synthetic seismograms. Cerveny et.al.[8] explain the main principles of dynamic ray tracing in ray centered coordinates, introduce the ray propagator matrix, summarize its applications and determine the geometrical spreading.
In the current paper all cases will be covered by introducing a scale factor in a single Algorithm. The technique used here gives faster results and takes less time compared to those of Cerveny et.al.[8] and Zednik [7]. They also use constant Gaussian beam, but variable Gaussian beam at the endpoint is used here.

2. GOVERNING EQUATIONS AND METHOD OF SOLUTION

The governing equations are given in reference [4]. But since there is no analytical solution for the general case, the following numerical method is used.
In a 3D-heterogeneous media the general wave displacement vector $\vec{w}$, in the vicinity of the central ray can be written in a compact form as;

$$\vec{w}(s,q_1,q_2,t) = \vec{w}_{\parallel}(s,q_1,q_2,t) + \vec{w}_{\perp}(s,q_1,q_2,t) \tag{1}$$

where $\vec{w}_{\parallel}$, $\vec{w}_{\perp}$ are the parallel (for P-wave) and normal (for S-wave) wave-displacements to the ray direction, respectively.
Components of equation (1) at time t with s as the arc length in the direction of the central ray at point O for high-frequency P and S-waves, $\vec{w}_P$ and $\vec{w}_s$ become:

$$\vec{w}_P(s,q_1,q_2,t) = Up\,\vec{t} + Ua_1\,\vec{e}_1 + Ua_2\,\vec{e}_2 \tag{2}$$

$$\vec{w}_s(s,q_1,q_2,t) = -Ua\,\vec{t} + Up_1\,\vec{e}_1 + Up_2\,\vec{e}_2 \tag{3}$$

Where, $(\vec{t},\vec{e}_1,\vec{e}_2)$ are the right-handed bases vectors at point O and (s,q_1,q_2) are the centeral ray curvilinear coordinate of point o in the vicinity of O (Figure 1).
The *principal*, Up and *additional*, Ua components of P and S rays are given by:

$$Up = E\,U_n \tag{4}$$

$$Ua = \eta E V(s) M\,U_n \tag{5}$$

where ;

$$E = \exp - i\omega\{(t - \int_0^s ds/[V(s)Q(s)]) + q^T M q/2\} \tag{6}$$

$$U_n = C\,U_m \tag{7}$$

$$C = \sqrt{[\tilde{\rho}\ \tilde{V}(s)\ |\tilde{J}|]/[\rho\ V(s)\ |J|]}\ R_{mn} \tag{8}$$

$$U_m = S_o \Big/ \sqrt{\rho\ V(s)|J|} \tag{9}$$

$$M = [M_{ij}] = [P/Q] \qquad i,j = 1,2 \tag{10}$$

where, M is the wavefield travel-time matrix of the complex second derivatives P and Q given in section-3 and can be computed by solving the dynamic ray tracing system, $Q(s)$ is the quality *(attenuation)* factor of the media, ω is the source angular velocity and $V(s)$ is the wave velocity along the ray. Tilda in equation (8) represents the wave discontinuities at the primary interface or variation at any point, i.e. properties of the layer at the generated or propagated ray side. ρ is the density, J is the Jacobian matrix given by Cerveny et al[2]. R_{mn}, is the modified version of matrix plane wave reflection and transmission coefficients at first order interface, but is one for second order interface[2].The computational procedures of the

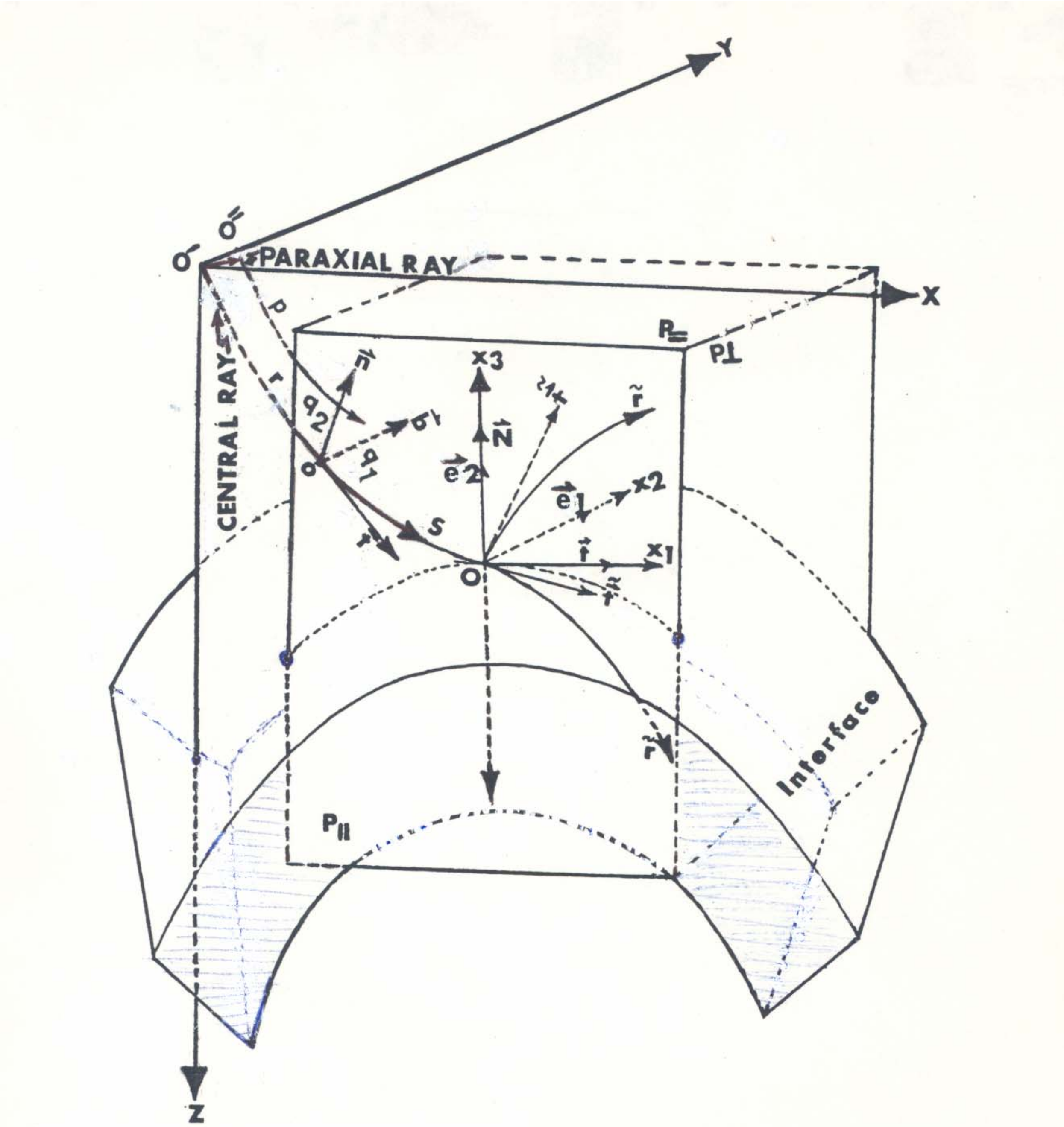

Figure 1. Global and local coordinate systems, central ray, its vicinity point *O*, first order interface and local coordinate (x_1,x_2,x_3) for 3-D seismic study of heterogeneous media.

dynamic ray tracing system with the corresponding initial conditions are given by Cerveny and Hron[9]. S_o *is source characteristic function* given as;

$S_0 = (\rho_0 V_0 SinD_0)^{1/2} g(t)$ for point source (11)

$S_0 = (\rho_0 V_0)^{1/2} g(t)$ for line source, (12)

where the source function is given by:

$$g(t) = Exp[-(2\omega^2 t^2 / d^2)]Cos(\omega t + \phi) \quad (13)$$

ϕ is phase function, d is a scale factor. The source could be either P or S-wave. There are no additional components for SH-waves. $U_m(s)$, and $U_n(s)$ are the incident and generated coefficient vectors corresponding to P, SV or SH-waves. η in equation (5) is a case factor to generate the following cases:

Case (1) $\eta = 0$ *and* $M = 0$: ART method of Cerveny et. al.[2].

Case (2) η ϕ 1 and $M = 1$: Extended Geometrical Ray Method[1].

Case (3) $\eta = 1$ and $M = [real]$: Central Ray Method [8].

Case(4) $\eta > 0$ and $M = [complex]$: Gaussian Beam Method [4].

Case (5) $\eta > 0$ and $M = [real]$: Paraxial Ray Approach[5].

In this paper the governing equations (4) and (5) are solved for case (3) based on variable super-position of Gaussian beams.

3. COMPUTATION OF THE JACOBIAN MATRIX AND RAY TORSION

The geometrical spreading of a wavefront can be defined in terms of Jacobian matrix J, of the transformation from the local cartesian coordinate into central ray coordinate system,

$$J = [\partial(s, q_1, q_2)/\partial(\varphi, \gamma_1, \gamma_2)]/V \quad (14)$$

Where, γ_1 *and* γ_2 are the ray parameters. φ denotes the eikonal function along the central ray, given as;

$$\varphi = 1/2 \quad \omega\, K_\omega(s)\, q^2 / V(s) \quad (15)$$

$$q^2 = q_1{}^2 + q_2{}^2 \quad (16)$$

The Jacobian matrix J is used to transfer the cross-sectional area of a ray tube dA from $q_1 - q_2$ to $\gamma_1 - \gamma_2$ plane, i.e.;

$$dA = |J|\, d\gamma_1 d\gamma_2 \quad (17)$$

Wesson[10], Cerveny[2] and Hubral[11] have introduced various methods to compute Jacobian determinant $|J|$. The most general one is to take partial derivatives of space coordinates, (q_1, q_2), and generalized impulses with respect to (γ_1, γ_2). This method was originally proposed by Popov and Psencik[12]. Equation (14) for two dimensional case can be represented by a second-order matrix instead of a third-order one, i.e.;

$$J(\varphi) = [\partial(q_1, q_2)/\partial(\gamma_1, \gamma_2)]/V \quad (18)$$

Then;

$$|J| = (q_{11} q_{22} - q_{21} q_{12})/V \quad (19)$$

Where;

$$q_{ij} = \partial q_i / \partial \gamma_j \quad i, j = 1,2 \quad (20)$$

In a general three-dimensional hetrogeneous media, when the ray torsion is not zero ($\tau \neq 0$), the dynamic ray tracing system can be written as[9];

$$\frac{dG}{d\varphi} = H\ G \quad (21)$$

Where, matrices H *and* G are given by:

$$G = \begin{bmatrix} Q \\ P \end{bmatrix}, \quad Q = [q_{ij}], \quad P = [p_{ij}],$$

$$H = \begin{bmatrix} 0 & \tau & V^2 & 0 \\ -\tau & 0 & 0 & V^2 \\ -V_{11}/V & -V_{21}/V & 0 & \tau \\ -V_{12}/V & -V_{22}/V & -\tau & 0 \end{bmatrix}, \quad (22)$$

for $i, j = 1,2$

where;

$$V_{ij} = \frac{\partial^2 V}{\partial q_i \, \partial q_j} \quad at\ (q_1 = q_2 = 0) \tag{23}$$

To solve for geometrical spreading, using the system (21), we must first know a point (*x,y,z*) on a central ray and the angles $\hat{I}$ *and* $\hat{D}$ defining the direction of the tangent $\vec{t}$. Angles $\hat{I}$ *and* $\hat{D}$ can be determined numerically using the eikonal ray tracing system;

$$\begin{aligned}
dx/d\varphi &= V\ Sin\hat{D}\ Cos\hat{I} \\
dy/d\varphi &= V\ Sin\hat{D}\ Sin\hat{I} \\
dz/d\varphi &= V\ Cos\hat{D} \\
d\hat{I}/d\varphi &= (V_x\ Sin\hat{I} - V_y\ Cos\hat{I})/Sin\hat{D} \\
d\hat{D}/d\varphi &= V_z\ Sin\hat{D} - (V_x\ Cos\hat{I} + V_y\ Sin\hat{I})\ Cos\hat{D}
\end{aligned} \tag{24}$$

Where;

$$V_x = \frac{\partial V}{\partial x}, \quad V_y = \frac{\partial V}{\partial y}, \quad V_z = \frac{\partial V}{\partial z} \tag{25}$$

If the coordinate system ($\vec{e}_1, \vec{e}_2$) does not rotate around the central ray (i.e. $\tau = 0$), then equation (21) is computationally faster than when it rotates (i.e. $\tau \neq 0$). The solution accuracy of the equation (21) can be checked by residual factor *F* given as;

$$(F = q_{11}p_{12} - q_{22}p_{21} + q_{21}p_{22} - q_{12}p_{11}) \tag{26}$$

F takes values between zero and one. If *F* is zero the solution is exact.

The initial conditions for the equation (21) are:

a.for the point source;

$$Q = [0], \quad P = \begin{bmatrix} -1/V_0\, SinD_0 & 0 \\ 0 & -1/V_0 \end{bmatrix} \tag{27}$$

b.for a line source;

assuming locally homogeneous medium in the vicinity of the source along $\vec{e}_1$,

$$Q = \begin{bmatrix} 1 & 0 \\ 0 & 0 \end{bmatrix}, \qquad P = \begin{bmatrix} 0 & 0 \\ 0 & -1/V_0 \end{bmatrix} \tag{28}$$

c-for a continuous ray(general case);

$$Q = Q_0, \quad P = P_0 \tag{29}$$

Subscript 0 means any initial condition at source.

The computational procedure would be much more complicated if the velocity changes across an interface of the first or second order.

To compute the Jacobian matrix, *J*, along the central ray of a generated wave, the initial conditions must be known at the boundaries. The relation between (Q,P) and $(\widetilde{Q},\widetilde{P})$ depends on the orientations of the vectors $(\vec{e}_1,\vec{e}_2)$ at the point of incidence on the interface (*O*). Let the local cartesian coordinate system (x_1,x_2,x_3) at the point of incidence be such that, x_3-axis is perpendicular to the interface, x_1-axis lies in the plane of incidence (Figure 1).

Take $\vec{e}_1$ along the x_2-axis and $\vec{e}_2$ the x_3-axis. Thus the initial conditions at first and second order interfaces become;

$$\begin{aligned}
&\widetilde{Q}_{i1} = Q_{i1}, \quad \widetilde{P}_{i1} = P_{i1} - 2Q_{i1}D_{22}R_1 - Q_{i2}\,S_2/Sin\theta \\
&\widetilde{Q}_{i2} = Q_{i2}\ Sin\widetilde{\theta}/Sin\theta, \\
&\widetilde{P}_{i2} = P_{i2}\,Sin\theta/Sin\widetilde{\theta} - Q_{i1}\ S_2/Sin\widetilde{\theta} - \\
&\qquad\qquad Q_{i2}\,S_1/Sin\theta\,Sin\widetilde{\theta}
\end{aligned} \tag{30}$$

The coefficients of the approximation equation of the non-planar interface $F(x_1, x_2, x_3) = 0$ in the vicinity of the point of incidence in the local coordinate system (x_1,x_2,x_3)can be written as:

$$D_{11}\ x_1^{\ 2} + 2D_{12}\ x_1x_2 + D_{22}\ x_2^{\ 2} - \varepsilon x_3 = 0 \tag{31}$$

$$\varepsilon = -Sign\ (F_x\ Sin\,D - F_y\ Cos\,D) \tag{32}$$

D is the angle between the tangent to the ray and the positive direction of the general x_3-axis at the point of incidence. ε in the interface equation (31) may be ± 1 depending on the orientation of normal to the curved boundaries. If $\varepsilon = -1$ as calculated from equation (32) then normal to the interface is in the positive x_3-direction, (i.e. interface is convex). If $\varepsilon = +1$ as calculated from equation (32) then normal to the interface is in the negative x_3-direction, (i.e. interface is concave). The parameters in equations (27), (28) and (29) are;

$$D_{ij} = -1/2\left(F_{x_i x_j} / F_{x_3}\right), \quad F_{x_3} = \partial F/\partial x_i ,$$

$$F_{x_i x_j} = \partial^2 F/\partial x_i \partial x_j , \quad R_1 = 1/V\, Sin\theta - 1/\widetilde{V}\, Sin\widetilde{\theta}$$

$$S_1 = 2/V\ \ Cos\theta(L_2 Sin\theta - \widetilde{L}_2 Sin\widetilde{\theta}) + 2D_{11}R_1 + (V_s - \widetilde{V}_s)\left(Cos\theta/V\right)^2 ,$$

$$S_2 = 1/V(L_1 - \widetilde{L}_1)Cos\theta + 2D_{12}R_1 ,$$

$$L_i = V_i/V , \qquad i = 1,3 \tag{33}$$

$$V_s = V_{x_1} SinD + V_{x_3} CosD$$

$$V_{x_i} = \partial V/\partial x_i \tag{34}$$

$$V_{ij} = \partial^2 V/\partial x_i \partial x_j$$

θ *and* $\widetilde{\theta}$ are the angles between the positive direction of the local x_1-axis and the tangential to the ray of the incident and generated waves, respectively. The angles are defined positively clockwise from the local x_1-axis, where they are related to the acute angles between the local x_3-axis and tangential to the corresponding ray.
The components of the unit normal to the non-planar interfaces can be computed using the phase matching methods[9] and [1].

4. MODELLING EXAMPLES

To show the applicability and reliability of the Central Ray Method in laterally as well as vertically heterogeneous media two computer packages (CRM-SSP and CRM-VSP) are written based on the above formulas and their flowcharts are shown in Figure 2.
Examples for both surface and vertical seismic profile data are considered.
Flowchart illustrates the procedure for iterative modeling used to compare a synthetic section and a real seismic data.

Case study I: Surface Seismic Profiling (SSP)
The P-wave point source and the receivers are located near the earth's surface while the direct wave has been omitted. Synthetic seismograms are computed for a constant Poisson's ratio ($\sigma = 0.25$). The distortion of waveforms due to recording equipment is not taken into account. The converged solution obtained by CRM-SSP program is shown in Figures 3 and 4 as follows;
*The obtained model and ray diagram in Figure 3a,
*The stacked seismic section (real data) in Figure 3b,
*The superimposed section (Figure 3c) of the records illustrating the obtained seismic section in Figure 3b,
*The NMO & STACK in Figure 3d,
*The MIGRATED section after stack in Figure 3e,
*The twenty four computed synthetic seismic records in Figure 4.
The real data and synthetic sections are compared in Figure 3a which shows very good approach to the geometrical model**.**

Case study II: Vertical Seismic Profiling (VSP)
This part deals with modelling of VSP synthetic used for interpretation of VSP seismic data. The seismic source is located at the earth's surface and the receivers are located in borehole. In this example the explosive point source is located 10 ft below the earth's surface. Three differen truns are given in a-500, b-900 and c-1500 feet from the borehole.
The converged solution obtained by CRM-VSP applied to an 80 degree dipping fault zone for source locations a-500, b-900 and c-1500 are summarized in Figures 5 and 6 as follows;
- The final fault model and its corresponding model, the source, the 30 receivers locations and the ray diagram in Figure 5,
- The synthetic VSP model computed using ray tracing program package showing primary reflection branches from horizons (1,2and3), the first order multiples and direct arrivals in Figure 6,

The converged solution obtained by FDM-VSP applied to an 80 degree dipping fault zone for source locations a-500, b-900 and c-1500 are summarized in Figures 7 and 8 as follows;

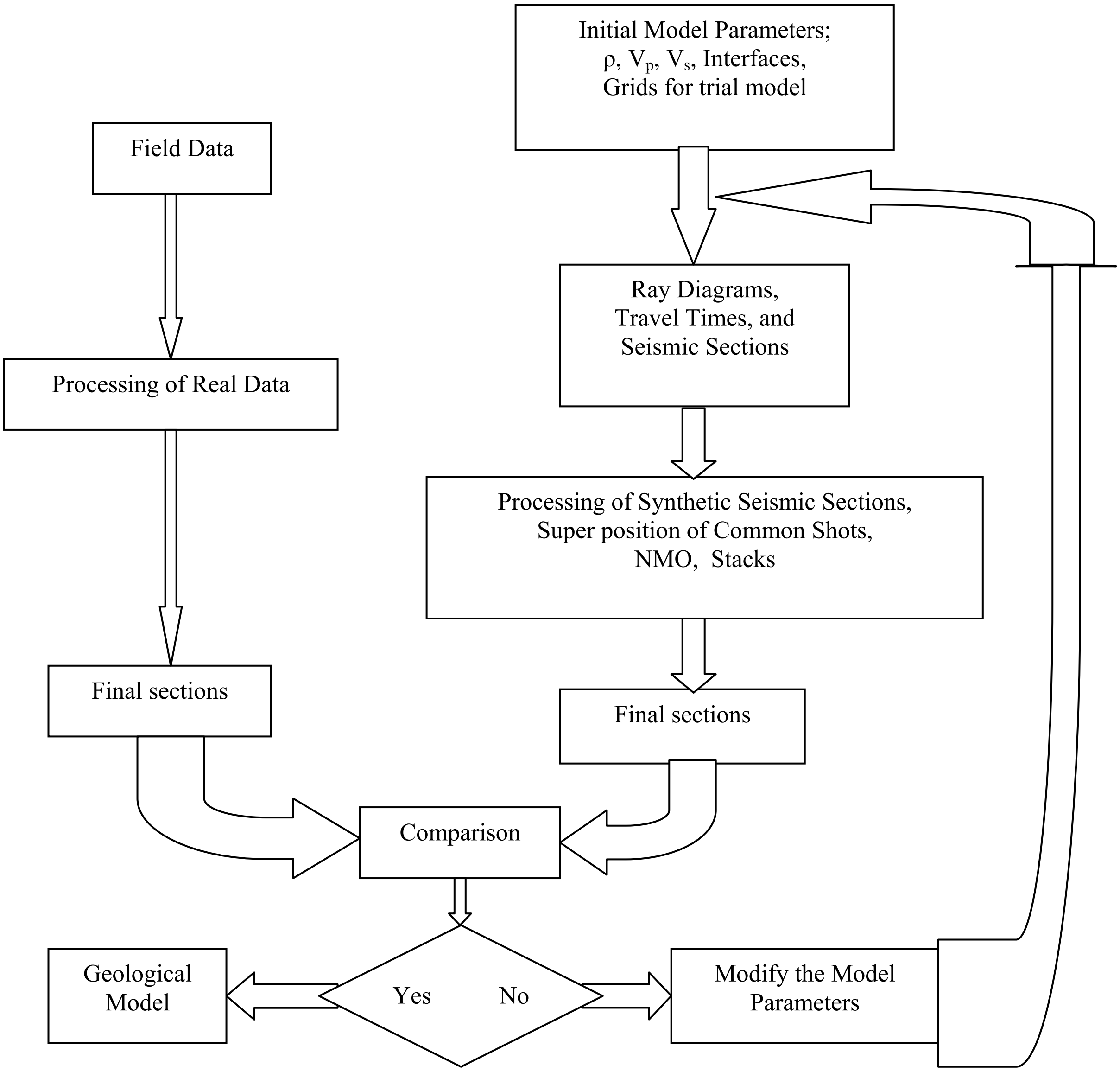

Figure 2. Flowchart for CRM-SSP, CRM-VSP & FD-VSP packages.

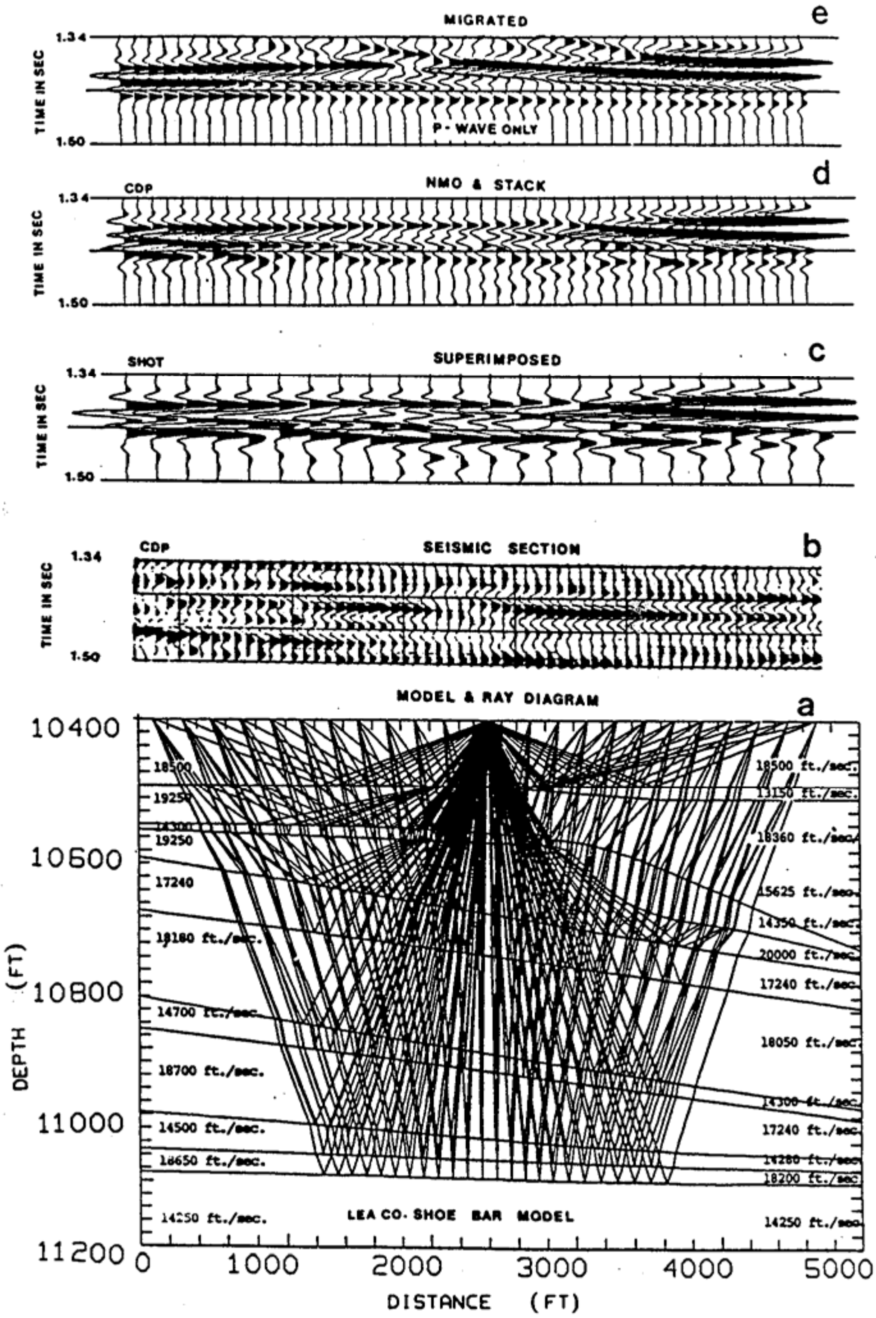

Figure 3. a-Final geological model, point source location, receivers, formation layers and the ray diagram.
b-The Seismic (stack-section).
c-Superimposed section.
d-NMO (Normal Move Out)and stack-section.
e- Migrated section

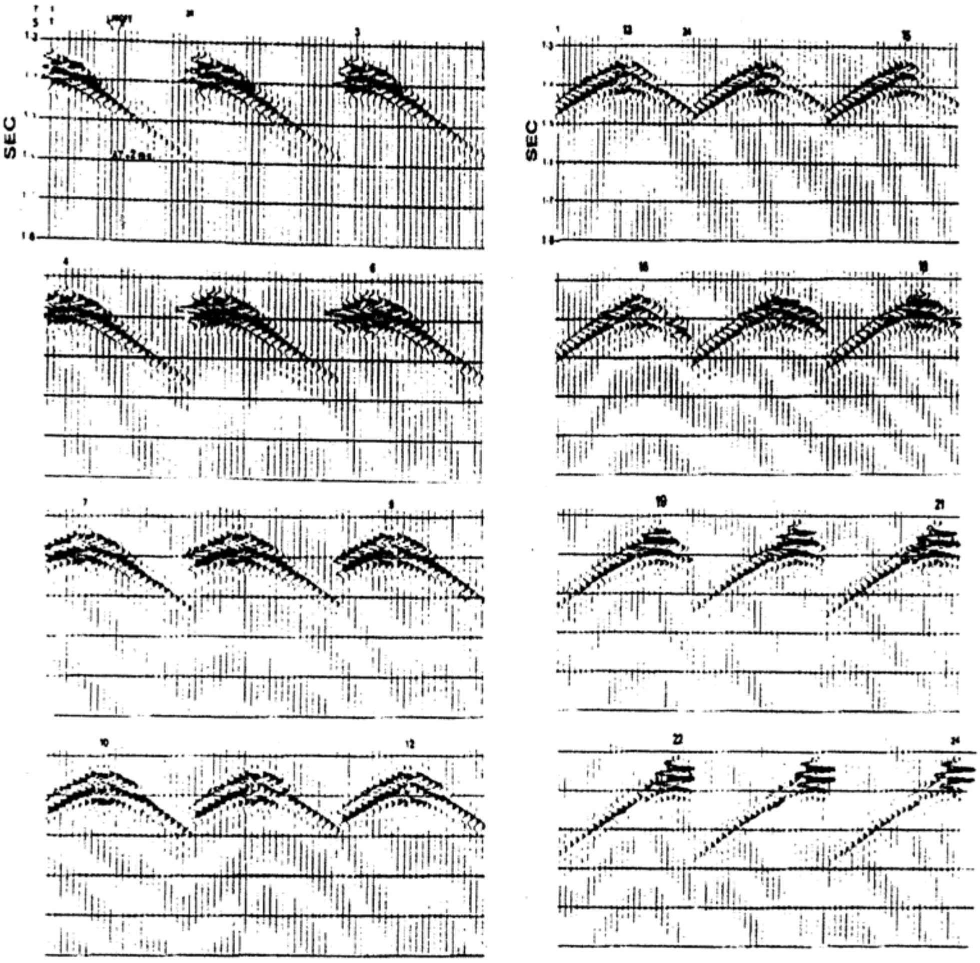

Figure 4. 24 synthtic seismic sections stacked to costruct superimposed section shown in Figure 3c.

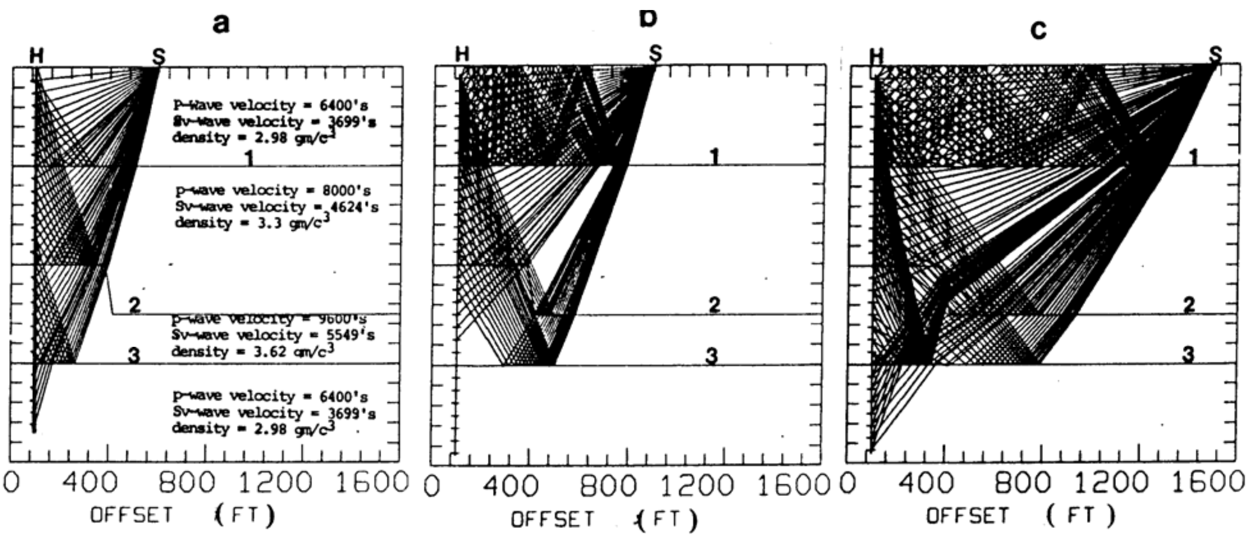

Figure 5. Final fault model, its corresponding rock parameters, 30 receivers locations, ray diagrams for the following source locations: a- 500’, b- 900’, c- 1500’

The finite difference and free surface multiple reflection waves, the up-coming and the down-going waves together with multiples in Figure 7,

- The superimposed structural model and wavefield snapshots (a-f) in Figure 8.

The VSP ray synthetic and finite-difference VSP sections are compared, which show very good agreement for three different source locations (near, intermediate and far-field offset).

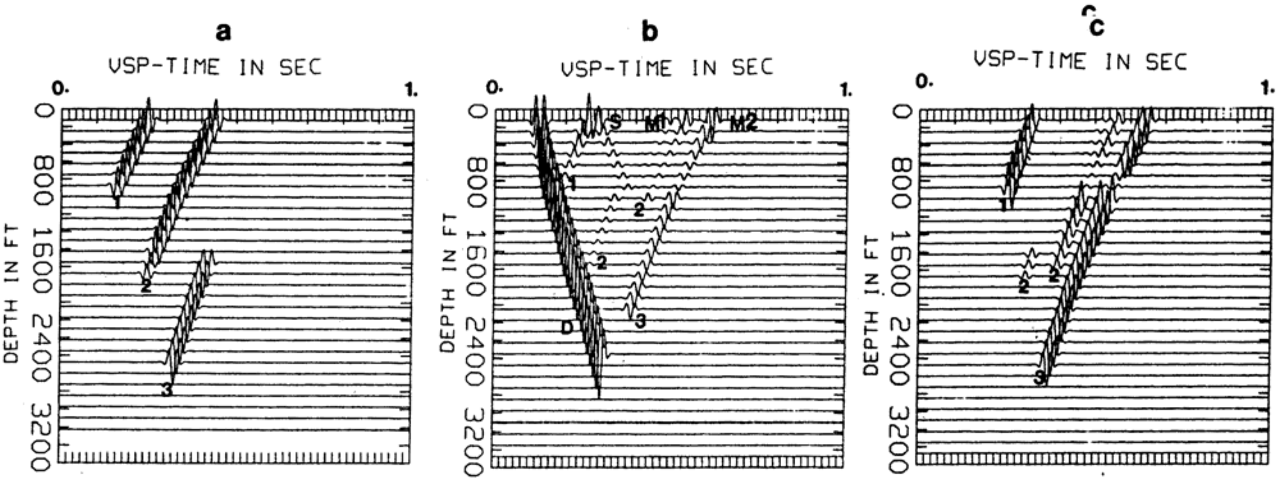

Figure 6. Ray VSP synthetic section for the following source locations; a-500’, b-900’and c-1500’

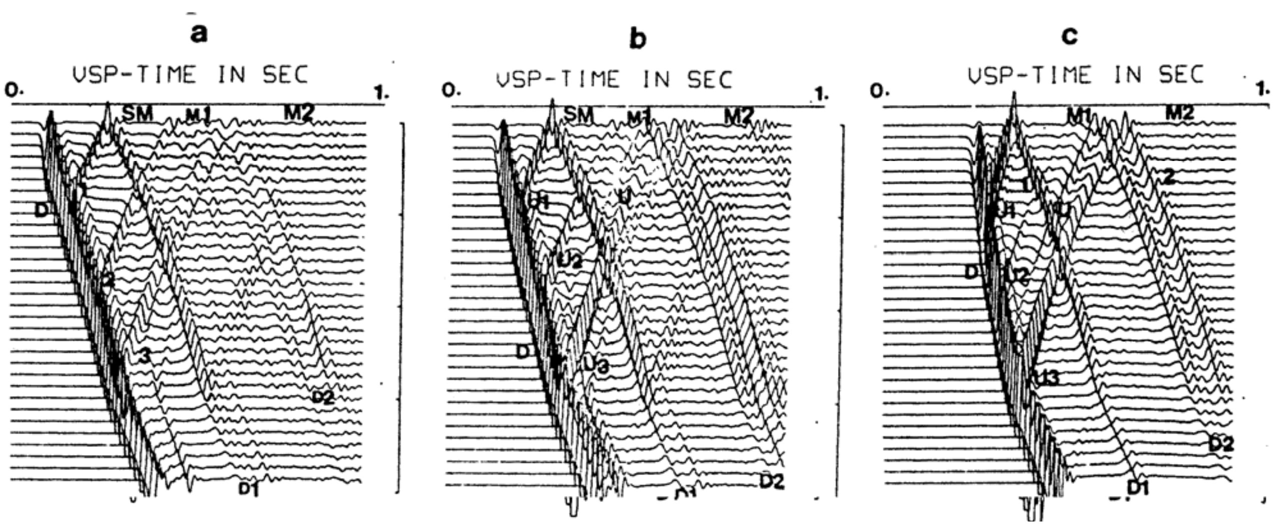

Figure 7. The finite difference VSP section for the following source locations; a-500’, b-900’and c-1500’.

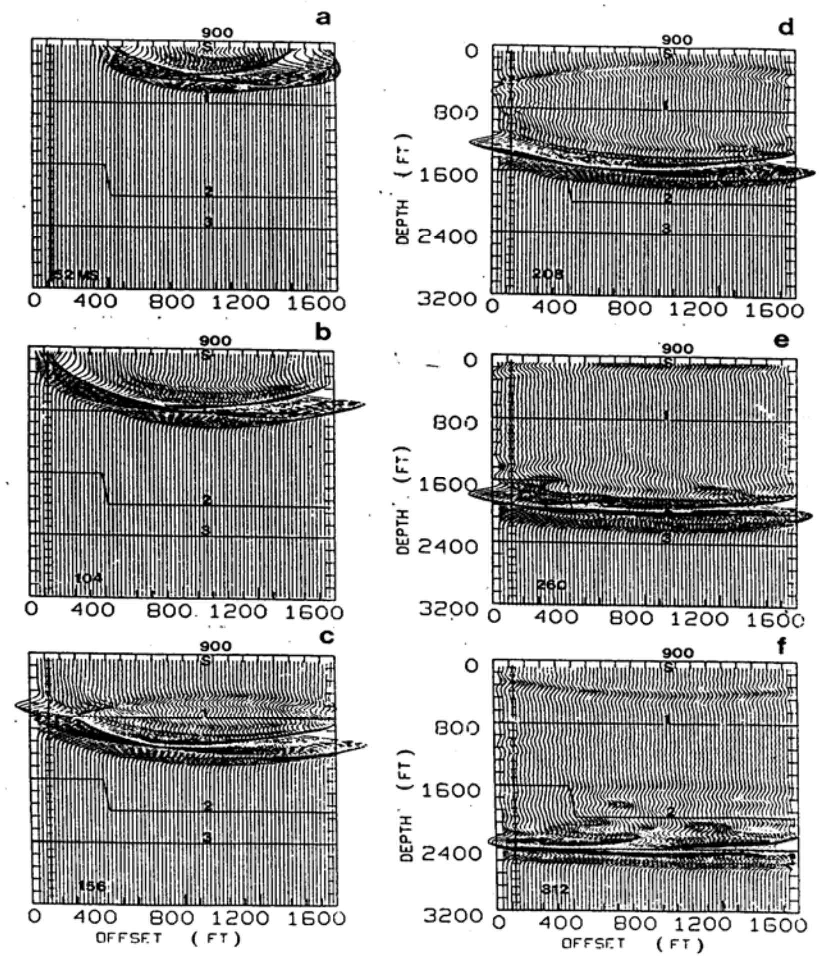

Figure 8. Superimposed structural model and wavefield VSP finite differenve snapshots(a-f), (Snapshot time step 52ms).

5.CONCLUSIONS

The correction for nonzero offset effects are done by applying conventional NMO and stack (Figure 3d).The aplication of finite difference migration to migrated synthetic section is slightly incorrect and does not show complete collapsing (Figure 3e). This may suggest that DMO (Dip Move Out) should be applied befor migration. The agreement between observed data and synthetic time branches is close (both with and without time migration). Therefore the superimposed section can be used with an initial model for a check before iterative modelling and to check the reliability of the method for the complex geologic models. The absorbing boundary conditions of Clayton and Engquist [13] are used in finite difference computations. The local stability condition used is $\Delta t \leq \Delta h / V\sqrt{2}$, Δh is mesh dimension. Figures 5-8, illustrate that the sensitivity of the seismograms to any structure are a function of source and receiver geometry. However, the methods reliability in the construction of waveforms are functions of velocity gradients in the model and the frequency present in the source. Comparison of Figure 6 and 7 show that the fault model can be constrained more precisely by the Ray method than the second-order finite-difference method. The effects, such as phase shift and Amplitude Versus Offset (AVO), interferences and lateral changes of the velocity model can be seen in the VSP's, computed by both the Ray method and the finite-difference program.

In conclusion , we can say that the conventional migration after stack is not always correct way to do time or structural migration (Figure 3e). For this type of geological structures (fractured or fault models) ray-equation migration may be useful.

6. REFERENCES

1. GhassemAL-Askari, M.K., *Seismic Body Waves in Laterally Inhomogeneous Media*, in *Department of Geological Sciences*. 1981, Southern Methodist University.
2. Cerveny, V., I. Molotkov, and I. Psencik, *Ray Method in Seismology*, ed. C.U. Press. 1977, Prague.
3. Cerveny, V. and R. Ravindra, *Theory of seismic head waves*. 1971, Toronto: University of Toronto Press.
4. Cerveny, V., *Expansion of a Plane Wave into Gaussian Beams.* Studia Geoph., et Geod., 1982. **26**: p. 120-131.
5. Cerveny, V., L. Klimes, and I. Psenick, *Paraxial Ray Approximation in the Computation of Seismic Wavefields in Inhomogeneous Media.* J. Geophys, 1984. **79**: p. 89-109.
6. Cerveny, V., M.M. Popov, and I. Psencik, *Computation of Wavefields in Inhomogeneous Media Gaussian Beam Approach.* Geophys. J. R. astr. Soc., 1980. **70**: p. 109-128.
7. Zednik, J., J. Jansky, and V. Cerveny, *Synthetic seismograms in radially inhomogeneous media for ISOP applications.* Computers & Geosciences, 1993. **19**(2): p. 183-187.
8. Cerveny, V., L. Klimes, and I. Psencik, *Applications of dynamic ray tracing.* Physics of The Earth and Planetary Interiors, 1988. **51**(1-3): p. 25-35.
9. Cerveny, V. and F. Hron, *The Ray Series Method and Dynamic Ray Tracing Systems for Three Dimensional Inhomogeneous Media.* Bull. Seism. Soc. Am., 1980. **70**: p. 47-77.
10. .Wesson, R.L., *A Time Integration Method for Computation of the Intensities of seismic Rays.* BSSA, 1970. **60**: p. 307-316.
11. Hubral, P. and T. Krey, *Interval Velocities from Seismic Reflection Time Measurement*. SEG Monogrph Sereis. 1980, Tulsa.
12. Popov, M.M. and I. Psencik, *Ray Amplitude in Inhomogeneous Media with Curved Interface.* Travaux-Inst., 1976. **454**.
13. Clayton, R.W. and B. Engquist, Absorbing Boundary Conditions for Acoustic and Elastic Wave Equations. BSSA, 1977. **67**: p. 1529-1540.